Gas transfer velocities of CO2 and CH4 in a tropical reservoir and its river downstream

Fabien Guérin, G. Abril, Dominique Serça, Claire Delon, S. Richard, Robert Delmas, A. Tremblay, L. Varfalvy

Gas transfer velocities of CO_2 and CH_4 in a tropical reservoir and its river downstream

Frédéric Guérin [a,b], Gwenaël Abril [b,*], Dominique Serça [a], Claire Delon [a], Sandrine Richard [c], Robert Delmas [a], Alain Tremblay [d], Louis Varfalvy [d]

[a] *Laboratoire d'Aérologie-OMP, Université Paul Sabatier, CNRS-UMR 5560, 14 Avenue E. Belin, F-31400 Toulouse, France*
[b] *Environnements et Paléoenvironnements OCéaniques (EPOC), Université Bordeaux 1 CNRS-UMR 5805, Avenue des Facultés, F-33405 Talence, France*
[c] *Laboratoire Hydreco, BP 823, F-97388 Kourou Cedex, Guyane Française, France*
[d] *Hydro-Québec, 75, Blvd R. Lévesque, Montréal, Québec, Canada*

We have measured simultaneously the methane (CH_4) and carbon dioxide (CO_2) surface concentrations and water–air fluxes by floating chambers (FC) in the Petit-Saut Reservoir (French Guiana) and its tidal river (Sinnamary River) downstream of the dam, during the two field experiments in wet (May 2003) and dry season (December 2003). The eddy covariance (EC) technique was also used for CO_2 fluxes on the lake. The comparison of fluxes obtained by FC and EC showed little discrepancies mainly due to differences in measurements durations which resulted in different average wind speeds. When comparing the gas transfer velocity (k_{600}) for a given wind speed, both methods gave similar results. On the lake and excluding rainy events, we obtained an exponential relationship between k_{600} and U_{10}, with a significant intercept at 1.7 cm h^{-1}, probably due to thermal effects. Gas transfer velocity was also positively related to rainfall rates reaching 26.5 cm h^{-1} for a rainfall rate of 36 mm h^{-1}. During a 24-h experiment in dry season, rainfall accounted for as much as 25% of the k_{600}. In the river downstream of the dam, k_{600} values were 3 to 4 times higher than on the lake, and followed a linear relationship with U_{10}.

Keywords: Tropical environment; Lake; River; Gas exchange; Wind speed; Rainfall

1. Introduction

In the context of global warming, the quantification of greenhouse gases emissions from the Earth surface is recognized as a priority. Recently, artificial reservoirs, particularly in the tropics, have been identified as significant CO_2 and CH_4 contributors to the atmosphere (Galy-Lacaux et al., 1999; Saint Louis et al., 2000; Abril et al., 2005). Owing to the microbial decomposition of soil and flooded biomass composed of primary tropical forest, tropical reservoirs emit large amounts of CO_2 and CH_4 to the atmosphere (Galy-Lacaux et al., 1999; Abril et al., 2005). A large fraction of the gaseous emissions occurs as diffusive fluxes from the surface of the artificial lakes or from the rivers downstream of the dam (Abril et al., 2005).

* Corresponding author. Tel.: +33 5 40 00 88 53; fax: +33 5 56 84 08 48.
E-mail addresses: f.guerin@epoc.u-bordeaux1.fr (F. Guérin), g.abril@epoc.u-bordeaux1.fr (G. Abril), serd@aero.obs-mip.fr (D. Serça), delc@aero.obs-mip.fr (C. Delon), sandr.richard@wanadoo.fr (S. Richard), delr@aero.obs-mip.fr (R. Delmas), tremblay.alain@hydro.qc.ca (A. Tremblay), varfalvy.louis@hydro.qc.ca (L. Varfalvy).

Diffusive CO_2 and CH_4 fluxes depend on the concentration gradient between the surface water and the atmosphere, which is mainly controlled by the gas concentration in the surface water, and by the gas transfer velocity, k. The diffusive CO_2 and CH_4 fluxes can either be measured directly or calculated from the surface water and air concentrations if k is known. Direct CO_2 and CH_4 fluxes measurements include three different techniques: the floating chambers (Frankignoulle et al., 1996a), the eddy correlation (McGillis et al., 2001) and the gradient flux techniques (Zappa et al., 2003). Indirect methods consist in measuring the gas concentration air–water gradient and determining k using deliberate tracers such as SF_6 (Wanninkhof et al., 1985) or $SF_6/^3He$ (Clark et al., 1994). In addition, measurements must be performed at a frequency that adequately reflects the temporal variations in the gas concentrations in surface waters and fluxes at inter-annual, seasonal and daily time scales. Recently, equilibrator techniques have been developed in order to measure continuously CO_2 and CH_4 concentrations in systems with rapid temporal variations like estuaries (Frankignoulle et al., 2001) and stratified tropical lakes (Abril et al., 2006). This allows continuous monitoring of gas concentrations variations in surface waters. When combined to an adequate parameterization of k, this would allow the calculation of accurate gas emission budgets.

In the present paper, we investigate the dependence of k on various meteorological parameters (wind speed, rainfall, and temperature) in an Amazonian tropical reservoir and its river downstream. We compare gas transfer velocities obtained by floating chamber and eddy covariance measurements of CO_2 and CH_4 fluxes performed at the same time on the same system. We establish experimental relationships of the gas transfer velocity against wind speed and rainfall and compared them with other studied lakes and rivers.

2. Materials and methods

2.1. Study site

The Petit-Saut dam was constructed on the Sinnamary River in the tropical forest of French Guiana 100 km upstream its mouth to the Atlantic Ocean. Relevant physical characteristics of the system are shown in Table 1. The reservoir started to be filled in January 1994 and covers 80 km of the Sinnamary River course. At its maximal level of 35 m (first reached in July 1995), 365 km^2 of un-cleared tropical forest are flooded. Owing to the differences between high and low water levels, the average surface of the reservoir is 300 km^2 (Table 1). Average residence time of waters is 5–6 months. The reservoir water body remains stratified throughout the year with a permanent thermocline around 6–8 m depth. Downstream of the dam, the Sinnamary River has an average depth of 4 m and is influenced by the tide with average amplitude of 0.5 m (Table 1).

2.2. Field experiments

Two field experiments were carried out in the reservoir in May and December 2003 during the wet and dry seasons. Intensive measurements of diffusive CO_2 ($n=211$) and CH_4 ($n=89$) fluxes were performed with floating chambers from a small boat at different sites on the reservoir, including open waters and flooded forest, and on the Sinnamary River and Estuary downstream of the dam. At each station, wind speed and air

Table 1
Characteristics of the Petit-Saut Reservoir

		Mean	Range
Meteorology	Wind speed ($m\ s^{-1}$)[a]	1.02	0–11.50
	Air relative humidity (%)[b]	86.76	38–107
	Annual precipitation (mm)[c]	2965	2156–4538
	Air temperature (°C)[b]	25.65	19.00–36.00
Lake	Surface (km^2)	300	260–365
	Volume ($10^9\ m^3$)	2.9	2.3–3.5
	Water discharge ($m^3.s^{-1}$)[d]	235	3–2431
	Turbined water discharge ($m^3\ s^{-1}$)	225	35–1957
	Depth (m)	10	0–35
	Surface water temperature (°C)[e]	30.42	27.50–33.70
	Thermocline depth (m)	7.5	7–8
Downstream river and estuary	Surface (km^2) <40 km	5	n.a.
	Surface (km^2) >40 km	17	n.a.
	Tidal range (m)	0.5	n.a.
	Depth	4	3–5
	Water temperature (°C)[f]	26.8	24.8–28.4

[a] Monthly average from August 2003 to June 2005.
[b] Monthly average from December 2002 to June 2005.
[c] Annual average from January 1991 to June 2005.
[d] Daily average of the water discharge entering the reservoir from June 1994 to June 2005.
[e] Monthly to bi-monthly average of measurements made at Roche Génipa (reference station since impoundment) from July 1995 to June 2005.
[f] Daily average at 40 km downstream the dam from July 1995 to June 2005.

temperature were measured at 1-m height, and surface water was sampled at 10 cm below the water surface for the determination of CO_2 and CH_4 concentrations. Surface water temperature was determined at the same depth than gas concentrations. In Dec. 2003, CO_2 fluxes were also measured by the Eddy Covariance technique ($n=35$) a few hundred meters upstream of the dam, during a 24-hour cycle. Chamber fluxes were measured at regular intervals on the distance of 20 m from the eddy covariance mast, for validation and intercomparison. During this 24 h-survey, gas concentrations in surface waters were monitored with an equilibrator.

2.3. Floating chambers measurements

Fluxes were measured with three different plastic floating chambers (FC) that were deployed simultaneously from a small boat that was left drifting during measurement to avoid creation of artificial turbulence. An exception was the 24-h cycle near the eddy covariance mast when chambers were deployed from an anchored boat. The FCs used in this study had walls extending 2–5 cm into the water column. Two small chambers (volume 20 L, surface 0.2 m^2, square design), connected to gas analyzers for CO_2 and CH_4 were deployed during 5 to 10 min, on 3 to 5 replicates. CO_2 was detected with a Non dispersive Infra Red analyzer (CIRAS-2SC, PP System), and CH_4 with a Fourier Transformation Infra Red analyzer (Gasmet DX-4010, Temet Instruments). The gas analyzers were calibrated with certified CO_2 and CH_4 gas standards at the beginning of each campaign (390 and 409 ppm for CO_2 and 90 ppm for CH_4, Gaz Spéciaux MEGS). In addition, the zero was checked automatically for the CIRAS-2SC and manually, everyday, with nitrogen for the Gasmet DX-4010. In order to avoid condensation problem into the sampling tube and/or inside the IRGA, the ambient air was passed through a water trap of sodium perchlorate. Fluxes were calculated from the slope of the partial pressure of the gas versus time, taking into account the air temperature. 80% of the CH_4 fluxes and 95% of the CO_2 fluxes were accepted ($r^2>0.90$) for k_{600} computations. The third chamber (FC-GC) was larger (volume 30 L, surface 0.20 m^2), with a circular design and equipped with a rubber stopper that allowed gas sampling with a syringe and needle. This chamber was deployed for 30 min on the Sinnamary River and 60 min on the reservoir, where fluxes are lower. Four 50-mL gas samples were taken at regular intervals (every 10 or 20 min) from the chamber after mixing the chamber volume by pumping with the syringe. The syringe was immediately connected to a N_2-preflushed 10-mL vial, leading to a dilution factor of 5/6. The CH_4 contents of the gas samples were then analyzed by means of a gas chromatograph (GC, Hewlett Packard HP 5890A) equipped with a flame ionization detector (FID). Fluxes were calculated from the linear regression of gas content versus time and 88% of the measurements were accepted ($r^2>0.90$).

2.4. Eddy covariance technique

The eddy covariance (EC) method is considered as the reference method for vertical flux scalar measurement (Beverland et al., 1996; McGillis et al., 2001). This method is based on the direct high frequency measurement of the two components of the vertical flux of a scalar: the vertical wind speed 'w' and the scalar itself, CO_2 or 'c' here. Flux comes as the integral of the product of the vertical wind speed fluctuation w' and of the scalar c':

$$F_c = \overline{w'c'} = \frac{1}{T}\int_0^T w'(t)c'(t)\,\mathrm{d}t = \frac{1}{T}f(t) \text{ with } f(t) = \int_0^T w'(t)c'(t)\,\mathrm{d}t \quad (1)$$

Although this method presents a number of advantages, the processing of raw data shows that data control is necessary to guarantee their quality for further use (Foken and Wichura, 1996; Affre et al., 2000). Such a control is relatively simple since all the turbulence functions involved are available and can be verified at all post-treatment steps (Mann and Lenschow, 1994).

Turbulence stationarity is one of the fundamental hypotheses that should be fulfilled when determining turbulent fluxes. The presence of low frequencies, which usually are not of local turbulent origin, but can be induced by the constraint of large-cell circulations or meso-scale events in the Atmospheric Boundary Layer (ABL), implies longer scale processes in the turbulent fluctuations. They can yield significant disturbances in flux evaluation. For this reason, and as defined in Affre et al. (2000), the contribution to $w'c'$ covariance is studied along the sample. The evolution of the integral function $f(t)$ defined in Eq. (1) is an indication of the quality of the integral flux which is given by $(f(T)-f(0))/T$. There is a second way to calculate the flux which is based on a statistical approach. In that case, the flux is no more calculated on the integral slope, but on the statistical slope deducted from the least mean squares.

The criterion presented here defines the sample homogeneity. This is done by calculating the mean slope

of the least mean square regression line. This slope corresponds to a statistical evaluation of the covariance $\sigma^2_{\mathrm{wcstat}}$. It takes into account all the function evolution and not only the extreme points as for the "classical" variance calculation. The homogeneity is quantified by evaluating the standard deviation σ_{wcreg} between $f(t)$ and the regression line. The CRS expressed in percentage (Eq. (1)), is then defined as the ratio of the standard deviation σ_{wcreg}, to the $w'c'$ covariance.

$$\mathrm{CRS} = 100\frac{2\sigma_{\mathrm{wcreg}}}{[f(t_2)-f(t_1)]} \approx 100\frac{2\sigma_{\mathrm{wcreg}}}{T\sigma^2_{\mathrm{wcstat}}} \quad (2)$$

It represents the error in the variance evaluation, and the higher the CRS is, the less homogeneous the sample is, and on the opposite, CRS tends to zero (small difference between the integral function $f(t)$ and the linear regression) for a linear $f(t)$ function and a homogeneous sample. Based on the statistical distribution, a cut-off limit was applied for fluxes with CRS higher that 20%.

Once the quality control was made with the CRS, time lags related to the time response of the scalar analyzer (and to the transfer through the tubing) was to be taken into account. In this case, the time lag is easily estimated through the calculation of the cross-correlation between w and c, as the time lag for which the cross-correlation shows a maximum. The flux is then calculated from the lagged functions. We found here a maximum correlation for a time lag of 9/5 s, consistent with the tubing length (4 m, 0.4×10^{-2} m inner diameter) and pump flow rate (10 L min^{-1}). Sampling tube effects were accounted by as proposed by Leuning and Judd (1996) and McGillis et al. (2001). We calculated a dimensionless cutoff limit proposed in the latter of these studies. This limit depends on the tubing length and inner diameter, the wind speed, the measurement height, the Reynolds number and the kinematic viscosity. We found that our system was capturing most of the turbulent flux as long as the wind speed was below about 8 m s^{-1}.

CO_2 fluxes were measured with the EC technique during the dry season, for a 24 h-period from December, 10 at 4:00 p.m. to December, 11 at 4:00 p.m. Experimental set up included a Gill® R1 3D sonic anemometer, a Licor® 6262 IR Gas analyser, calibrated, at the beginning of the experiment with certified gas standard (Air Liquide, 500 ppm), and a lab-made datalogger. 5 Hz logging of horizontal wind components (U, V), vertical wind component (W), temperature (T), CO_2 and H_2O data was performed on a 30 min basis, given, after quality control (CRS > 20%), a total of 35 (over 48) fluxes for subsequent flux calculation. The Sonic anemometer and the tubing were installed 2.1 m above the reservoir water level at the tip of a small flat island located 400 m south-east of the dam. Fetch ranged from 400 to 1500 m in all directions, excepted of wind coming from the south. A wind sector analysis showed that no samples were collected in this latter direction.

2.5. Gas concentration gradients

At each station, CO_2 surface concentration was measured by a headspace technique in 30-mL vials (headspace volume 15 mL) followed by a GC-TCD analysis. As described by Hope et al. (1995), this method is the most appropriate for acid, low ionic strength, organic rich waters as in Petit-Saut. Concentrations were computed with the solubility coefficient of Weiss (1974). CH_4 surface concentration was also measured by the headspace technique followed by the GC-FID analysis and surface concentrations were computed with the solubility coefficient of Yamamoto et al. (1976). During the 24-hour survey, the surface concentrations were measured in air equilibrated with subsurface water pumped from a depth of 20 cm using an equilibrator connected to a photo-acoustic gas analyzer (Abril et al., 2006). Atmospheric concentrations were obtained by GC-FID (CH_4 with FC-GC) and by the gas analyzers connected to the FCs at initial time of each flux measurements.

2.6. Meteorological variables

Wind speed and air temperature were measured with a portable anemometer (Kestrel 4000, accuracy: 3%) at 1-m height for all stations on the lake and the river. Wind speed at 10-m height (U_{10}) was recalculated using the Amorocho and DeVries (1980) formulation:

$$U_z = U_{10}\left[1-C_{10}^{1/2}\kappa^{-1}\ln(10/z)\right] \quad (3)$$

where C_{10} equals the surface drag coefficient for wind at 10 m (1.3×10^{-3}; Stauffer, 1980), κ equals the von Karman constant (0.41), and z the height of wind speed measurements (meter) above the water surface.

During the 24-hour survey near the dam in December 2003, a meteorological station (OTT HYDROMETRY sensors) installed on the dam at 10-m height above the water surface measured, at 1-min interval, the wind speed (accuracy: 3%), the rainfall rate (accuracy: 0.01 mm min^{-1}), the air temperature and relative humidity. Wind speed and rainfall rate were averaged over the duration of the flux measurement.

2.7. Calculation of the gas transfer velocity

The flux across an air–water interface can be formulated as follows:

$$F_{g,T} = \alpha k_{g,T} \Delta P \quad (4)$$

with

$$\Delta P = P_{w,g} - P_{a,g} \quad (5)$$

where $F_{g,T}$ is the flux at air–water interface for a given gas (g) at a given temperature (T), α is the solubility coefficient of the considered gas, $k_{g,T}$ is the gas transfer velocity (or piston velocity) for a specific gas at a given T, and ΔP the partial pressure gradient between water ($P_{w,g}$) and the overlying atmosphere ($P_{a,g}$).

To compare the exchange coefficient for different gases and at different water temperatures, the gas transfer velocity was normalized to a Schmidt number of 600 (Sc=600, for CO_2 at 20 °C) with the following equation (Jähne et al., 1987):

$$k_{600} = k_{g,T}(600/Sc_{g,T})^{-n} \quad (6)$$

where $Sc_{g,T}$ is the Schmidt number of a given gas at a given temperature (Wanninkhof, 1992). For the lake, we used n=2/3 for wind speed <3.7 m s^{-1}, and n=0.5 for higher wind speed (Liss and Merlivat, 1986; Jähne et al., 1987). In the turbulent river downstream, we used n=0.5 whatever the wind speed (Borges et al. 2004a).

3. Results and discussion

3.1. Description of the dataset

Three regions of the Petit-Saut system can be differentiated in terms of gas concentrations and fluxes: the reservoir surface (lake), the first section of the Sinnamary River from 0 to 40 km downstream of the dam, and the second section of the river, from 40 to 80 km, corresponding to the limit of the coast of the Atlantic Ocean. CO_2 and CH_4 fluxes measured at these different sites are shown in Table 2.

Surface waters of the lake were supersaturated in both studied gases with respect to the atmospheric equilibrium, with mean ΔpCO_2=3340±802 µatm and ΔpCH_4=81±76 µatm for both sampling periods. Resulting mean fluxes to the atmosphere were 103± 82 mmol m^{-2} d^{-1} and 4±6 mmol m^{-2} d^{-1} for CO_2 and CH_4, respectively. The large range of ΔpCO_2 and ΔpCH_4 for a given season (Table 2) were mainly due to the variety of sampling sites (e.g., flooded forest, open waters) and meteorological conditions. The Petit-Saut Lake can be destratified during high wind speed and rainfall periods (Abril et al., 2006). These short and dynamic phenomena can cause an increase of surface concentrations and partly explains why ΔpCH_4 are significantly higher in the wet season than in the dry season. For CO_2, only 3 surface concentrations were measured during the May campaign. Rainfall events were only sampled in Dec. 2003, when, in addition, wind speeds were higher (Table 2).

CO_2 and CH_4 diffusive fluxes along the first 40 km section downstream of the dam were the highest of the Petit-Saut whole system. The ΔpCO_2 were 4 to 10 times higher than at the lake surface and the resulting fluxes to the atmosphere were 10 times higher (Table 2). The ΔpCH_4 were 6 to 30 times higher than in the lake and the corresponding fluxes were one order of magnitude higher (Table 2). These high CO_2 and CH_4 concentrations in this section of the river originate from the reservoir hypolimnion (Galy-Lacaux et al., 1999; Abril et al., 2005). The fluxes to the atmosphere were very high due to very high

Table 2
Sampling dates and dataset

Site	Lake		River downstream (< 40 km)		River downstream (> 40 km)	
Sampling period	May 2003	December 2003	May 2003	December 2003	May 2003	December 2003
$F(CO_2)$ (mmol m^{-2} d^{-1})	113±90 (50)	99±79 (117)[a]	936±572 (24)	928±370 (20)	864±487 (11)	750±317 (13)
ΔpCO_2 (µatm)	1525±564 (3)	3390±694 (116)[a]	9275±1860 (10)	12857±648 (19)	8781±1632 (7)	10142±2290 (8)
$k_{600}(CO_2)$ (cm h^{-1})	2.34±1.59 (3)	2.93±2.12 (116)[a]	14.72±6.22 (10)	8.03±3.21 (19)	11.62±7.08 (7)	7.96±3.13 (8)
$F(CH_4)$ (mmol m^{-2} d^{-1})	6±7 (18)	2±2 (17)[b]	57±27 (15)	115±59 (21)	0.46±0.36 (8)	1.78±1.27 (10)
ΔpCH_4 (µatm)	122±86 (18)	37±24 (17)[b]	754±413 (10)	1167±597 (18)	3.55±1.07 (8)	6.07±4.54 (6)
$k_{600}(CH_4)$ (cm h^{-1})	3.13±2.29 (18)	5.10±6.30 (17)[b]	10.06±5.60 (10)	8.31±4.31 (18)	12.06±6.06 (8)	20.32±9.14 (6)
U_{10} (m s^{-1})	2.48±2.62	1.84±1.28	2.21±0.96	1.05±0.89	1.88±0.76	3.23±1.29

[a] Average with 28 values during rainy event. For these data, $F(CO_2)$ range from 29.56 to 449.13 mmol $m^{-2}.d^{-1}$, k_{600} from 0.81 to 13.37 cm h^{-1} and rainfall rates from 0.6 to 25.26 mm h^{-1}.

[b] Average with 5 values during rainy event. For these data, $F(CH_4)$ range from 1.75 to 6.95 mmol $m^{-2}.d^{-1}$, k_{600} from 2.59 to 28.35 cm h^{-1} and rainfall rates from 2.40 to 36.00 mm h^{-1}.

Table 3
Comparison of the CH_4 fluxes obtained by the two different floating chambers and the CO_2 fluxes obtained by eddy covariance and floating chamber measurements

Gas	Site	FC-IRGA (20L)	FC-GC (30L)	EC
CH_4	Lake	5.34 (0.6–29.4) $n=10$	4.64 (0.2–23.5) $n=12$	
	River downstream (0–40 km)	95.1 (47.7–161.2) $n=7$	81.3 (29.5–144.4) $n=7$	
	River downstream (40–80 km)	1.41 (0.15–3.3) $n=4$	0.90 (0.4–2.6) $n=6$	
CO_2	Lake	134.97[a] (21.76–449.13) $n=40$		90.76[#] (29.80–371.32) $n=35$

[a] Floating chamber with an Infra red gas analyzer with associate mean wind speed of 1.65 m s^{-1} (0.12–6.14 m s^{-1}) and rainfall rates of 5.25 mm h^{-1} (1.00–25.26 mm h^{-1}).
[#] Eddy covariance with associate mean wind speed of 1.52 m s^{-1} (0.18–3.87 m s^{-1}) and rainfall rate of 3.40 mm h^{-1} (0.60–8.64 mm h^{-1}).

concentrations, together with high gas transfer velocities in the downstream river (see Table 2 and next section).

In the second section of the river (>40 km), ΔpCH_4 and CH_4 fluxes decreased rapidly (Table 2), due to the loss of CH_4 by emission to the atmosphere and aerobic oxidation (Galy-Lacaux et al., 1999). In the >40 km river section, CO_2 fluxes were on average for the two campaigns 750 mmol m^{-2} d^{-1} (Table 2). Surface pCO_2 and ΔpCO_2 were close or higher than 10000 μatm all along the river, except at the limit of the coast, where it was around 6000 μatm. These high pCO_2 along the whole estuary are attributed to an intense mineralization of organic matter originating from the reservoir (Abril et al., 2005).

3.2. Comparison of techniques

Fluxes obtained with floating chambers have been dismissed by several workers (Liss and Merlivat, 1986; Marino and Howarth, 1993; Raymond and Cole, 2001; Matthews et al., 2003). Two main contradictory critics were formulated. On one hand, FC is considered to increase the turbulence at the water surface (Marino and Howarth, 1993; Raymond and Cole, 2001). However, as described by Frankignoulle et al. (1996a), drifting with the water masses, as done in our study, limits such disturbance. Artificial turbulence can also be created when the FC walls do not extend below the water surface. In such case, the chamber drifts above the water surface which can generate gas fluxes up to five times higher in comparison to FCs with wall extensions into the water (Matthews et al., 2003). This artifact becomes very important at low wind speed, as shown by Matthews et al. (2003), who compared FCs with wall not extending into the water with an SF_6 addition during a period at wind speeds <1 m s^{-1}. Eugster et al. (2003) compared 8 one-hour measurements by FC with 16 half-an-hour EC samples in a lake, and concluded that the FC gave CO_2 fluxes more than double than the EC fluxes. However, at the exception of samples taken during heating periods (3 FC fluxes), fluxes derived from FC measurements were very similar to those computed with the Cole and Caraco (1998) k-wind relationship and a surface-renewal model including the wind effect and the heat loss between the

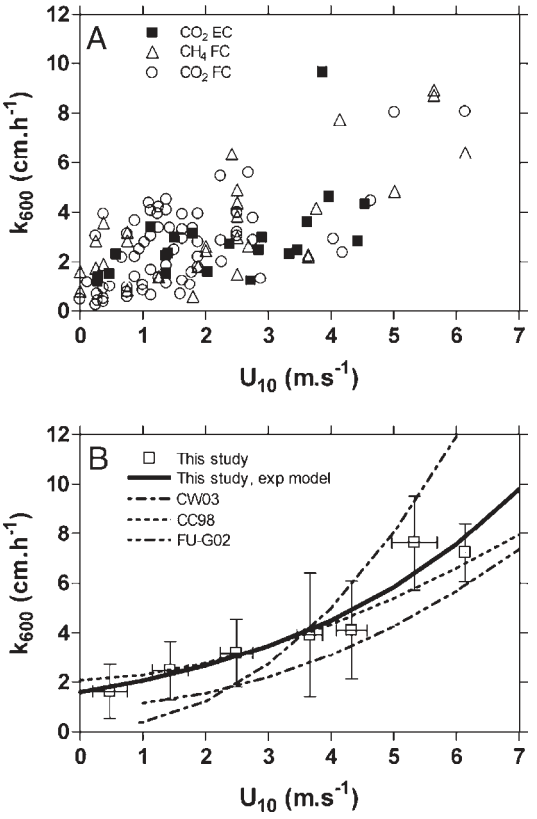

Fig. 1. Relationship between k_{600} and U_{10} at the Petit-Saut Lake. (A) Normalized gas transfer velocities, k_{600}, plotted against mean wind speed recalculated at 10 m (U_{10}) at the lake surface computed from CO_2 fluxes measured with floating chambers (open circle) and eddy covariance (solid square) and from CH_4 fluxes measured with floating chambers (open triangle). (B) All data were considered and k_{600} were averaged over wind speed bins of 1 m s^{-1}. The solid line corresponds to the best fit (exponential) for this study relationship, the long-dashed line corresponds to Cole and Caraco (1998) power relationship (CC98), the short-dashed line corresponds to the Crucius and Wanninkhof (2003) power relationship (CW03), and the dashed-dotted line to the Frost and Upstill-Goddard (2002) power relationship (FUG02).

water and the atmosphere (Crill et al., 1988; MacIntyre et al., 1995). The comparison of the two methods by Eugster et al. (2003) must therefore be taken with caution because it is based on few data, including net positive air-to-water CO_2 fluxes by EC while pCO_2 in the water was above the atmospheric concentration. These unexplained air-to-water fluxes significantly lowered the mean efflux values from EC and created most of the discrepancy between the two methods.

The second critic formulated was that FCs isolate the water surface from the influence of wind (Liss and Merlivat, 1986). However, the gas exchange is controlled by the turbulence in the aquatic boundary layer (Liss and Slater, 1974; McGillis et al., 2001; Kremer et al., 2003a) and if these conditions are determined over an area that is large enough relative to that influenced by the FC, the method could be reliable (Jähne et al., 1987). The disturbance of the FC on the wind speed boundary layer was tested experimentally by Kremer et al. (2003a), who measured O_2 fluxes using a FC with a fan to generate air turbulence and using a control FC in parallel. Under moderate wind conditions (1.6–3.4 m s^{-1}), the presence of the fan increased the fluxes by only 2% to 12%; such error is below classical sampling variability. Kremer et al. (2003a) also reported a series of experiments comparing the FC with mass balance approaches of O_2, ^{222}Rn, and ^{3}He in various experimental setting. Fluxes based on FC technique agreed with the other direct methods within 10% to 30%. Furthermore, Borges et al. (2004b) show that k values determined by Frankignoulle et al. (1996b) in coral reefs fits within k-wind parameterizations from open ocean, hence, going against the recurrent argument that FC artificially enhances the fluxes. The recent work of Borges et al. (2004a) in tidal estuaries also indirectly validates the reliability of the floating chamber with other methods showing the strong dependency of k_{600} with wind speed and water current velocity.

In the present study, the two FCs used to measure CH_4 fluxes were not deployed for the same duration time (30–60 min versus 5–10 min) due to differences of volume and detection sensitivity (GC-FID versus IRGA), and thus, can not be compared individually. In Table 3, we compare the CH_4 fluxes obtained for the lake and the river downstream with the two FCs for both campaigns. The differences between these two chambers were within 7% at the lake surface, 15% in the first 40 km river section and 33% in the second river section (>40 km) (Table 3). During the 24-h survey we measured concomitant CO_2 fluxes by EC and FC. The comparison of individual measurements is also difficult for two reasons: first, the fluxes are measured during 30 min for the EC and only during 5–10 min for FC which results in different average turbulent conditions; second, EC and FC measurements do not correspond to the same space scale: our EC integrates flux from a surface of 4 10^4 m^2 (Businger, 1986) compared to <1 m^2 for the FC. Nevertheless, average CO_2 fluxes during the same 24-h period were 91±73 mmol m^{-2} d^{-1} and 135±90 mmol m^{-2} d^{-1} for the EC and the FC techniques respectively (Table 3). The difference between these two mean fluxes was within 30%, in the generally accepted range of error for this type of experiment (Kremer et al., 2003a). In our case, these discrepancies can be explained by the difference of average meteorological conditions during the measurements. Respectively for the EC and FC measurements, mean wind speeds were 1.5 m s^{-1} and 1.7 m s^{-1}, and mean rainfall rates were 3.4 mm h^{-1} and 5.3 mm h^{-1} (Table 3).

Table 4
Correlation function between the gas transfer velocity (k_{600}, cm h^{-1}) and the wind speed at 10 m height (U_{10}, m s^{-1}) and rainfall rates (R, mm h^{-1}) in the Petit-Saut Reservoir and in the tidal river downstream based on unbinned and bin-averaged data (k_{600} data were averaged over wind speed bins of 1 m s^{-1})

		Function	Equation	r^2	p	n
Lake (k_{600} vs. U_{10})	Unbinned	Linear	$k_{600}=0.90\pm0.09.U_{10}+1.29\pm0.21$	0.46	<0.0001	121
		Power	$k_{600}=1.69\pm0.27+0.33\pm0.18.U_{10}^{1.59\pm0.32}$	0.47	<0.0001	121
		Exponential	$k_{600}=1.61\pm0.13.e^{0.26\pm0.02.U_{10}}$	0.48	<0.0001	121
	Bin average	Linear	$k_{600}=1.05\pm0.17.U_{10}+0.74\pm0.67$	0.88	0.0017	7
		Power	$k_{600}=1.76\pm0.77+0.23\pm0.32.U_{10}^{1.78\pm0.72}$	0.91	0.0107	7
		Exponential	$k_{600}=1.66\pm0.34.e^{0.26\pm0.04.U_{10}}$	0.92	0.0030	7
Lake (k_{600} vs. R)	Bin average	Linear	$k_{600}=-1.81\pm1.52+0.66\pm0.10R$	0.84	0.0002	10
Tidal river (k_{600} vs. U_{10})	Unbinned	Linear	$k_{600}=2.47\pm0.50.U_{10}+5.87\pm1.13$	0.23	<0.0001	86
		Power	$k_{600}=5.41\pm1.90+3.01\pm1.92.U_{10}^{0.88\pm0.38}$	0.23	< 0.0001	86
		Exponential	$k_{600}=6.97\pm0.85.e^{0.20\pm0.04.U_{10}}$	0.22	< 0.0001	86
	Bin average	Linear	$k_{600}=2.70\pm0.52.U_{10}+5.37\pm1.51$	0.90	0.0140	5
		Power	$k_{600}=6.42\pm3.17+1.68\pm2.55.U_{10}^{1.27\pm0.88}$	0.90	0.0499	5
		Exponential	$k_{600}=6.59\pm1.01.e^{0.22\pm0.04.U_{10}}$	0.91	0.0114	5

3.3. Wind effect

In the Fig. 1A the k_{600} obtained on the lake with the EC and the FC are plotted versus the wind speed at 10 m (U_{10}). The k_{600} values during rainy events are not shown in this figure. It can be seen that, besides some general scatter in the data, both methods fall within the same range for a given U_{10}. Similarly, the $k_{600}(CO_2)$ and $k_{600}(CH_4)$ obtained by FC are consistent on the lake. At the lake surface, the gas transfer velocities obtained by FC (2.2 ± 1.4 cm h^{-1} and 1.9 ± 1.0 cm h^{-1}, respectively for $k_{600}(CO_2)$ and $k_{600}(CH_4)$) are more scattered and/or a little bit higher on average than the k_{600} obtained by EC (2.0 ± 0.8 cm h^{-1}) for $U_{10} < 2$ m s^{-1}. For wind speed ranging from 0.1 to 4.6 m s^{-1}, we found a mean k_{600} of 2.6 ± 1.6 cm h^{-1} ranging from 0.7 to 9.7 cm h^{-1} with the EC technique, and the $FC(CO_2)$ gave a k_{600} of 2.4 ± 1.5 cm h^{-1} and $FC(CH_4)$ gave $k_{600} = 2.8 \pm 1.7$ cm h^{-1}. Note also that FC measurements were made in different locations of the lake with different water current velocities (max 30 cm s^{-1} in the lake) and depths that can influence the k_{600} and explain the scatter observed in our data (Fig. 1A). In order to reduce uncertainties (Cole and Caraco, 1998; McGillis et al., 2001; Borges et al., 2004a), data were averaged over wind speed bins of 1 m s^{-1} (Fig. 1B). Various parameterization functions (linear, exponential, and power) have been used in the literature; based on statistical analyses (r^2 and p values), the exponential model was the most appropriate for Petit-Saut Reservoir (Table 4). At very low wind speed (<3.7 m s^{-1}), we observe a weak dependency of k_{600} with wind speed, consistent with several studies in lakes, oceans and wind tunnels (Wanninkhof et al., 1985; Liss and Merlivat, 1986; Cole and Caraco, 1998; Wanninkhof, 1992; Frost and Upstill-Goddard, 2002; Crucius and Wanninkhof, 2003). The slope of the relationship was 0.7 cm h^{-1}/m s^{-1} for wind speed < 3.7 m s^{-1}, similar to what is found in Liss and Merlivat (1986), and 1.7 cm h^{-1}/m s^{-1} at higher wind speed. In addition, the intercept at zero wind speed was 2 to 3 times higher than in several previous studies (Wanninkhof et al., 1985; Frost and Upstill-Goddard, 2002; Crucius and Wanninkhof, 2003), except the one of Cole and Caraco (1998) on Mirror Lake determined by SF_6 addition. This could be due to thermal effects. The effect of evaporation (warm layer) and condensation (cool skin) on the gas transfer velocity was tested in a wind tunnel (Liss et al., 1981) and over the Pacific Ocean (Ward et al., 2004). These authors have shown that the gas transfer velocity can be enhanced by 4% to more than 30% under evaporative condition ($T_{water} > T_{atm}$) due to the destabilization of the near surface water. Frost and Upstill-Goddard (2002) measured gas transfer velocity by SF_6 evasion from a temperate reservoir ($\Delta T = T_{water} - T_{atm} = -1.4$ °C) and found a k_{600} lower than 1 cm h^{-1} for very low wind speed (Fig. 1B). In tropical environments, water is generally warmer than the overlying air above the water surface. In a tropical floodplain, MacIntyre et al. (1995) showed that more than 50% of the CH_4 fluxes observed by Crill et al. (1988) could be explained by convective cooling at very low wind speeds (<2 m s^{-1}). Anderson et al. (1999) presented k_{600} values ranging from 1 to 15 cm h^{-1} for wind speed ranging from 2 to 8 m s^{-1} derived from CO_2 fluxes measured with the EC technique at a woodland lake surface. For a given wind speed, k_{600} varied from 60% to 90%. They found the

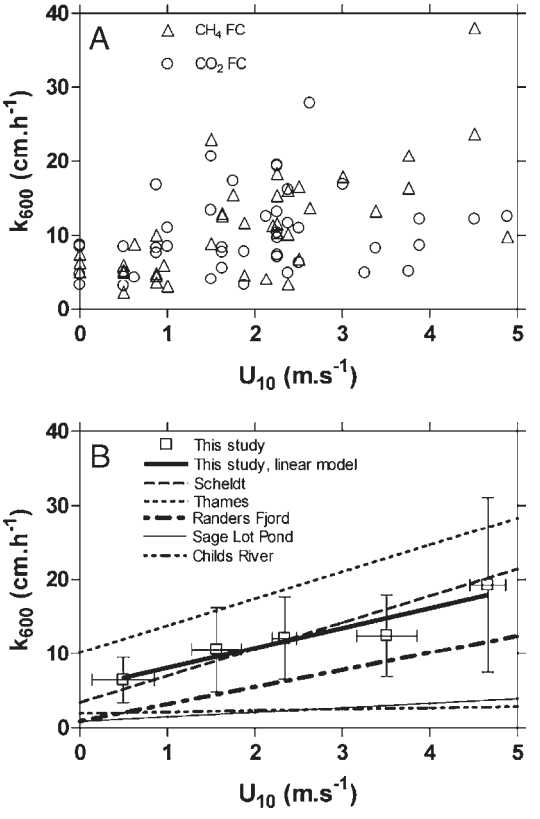

Fig. 2. Relationship between k_{600} and U_{10} on the Sinnamary River and Estuary. (A) Normalized gas transfer velocities, k_{600}, plotted against mean wind speed recalculated at 10 m (U_{10}) at the downstream river surface computed from CO_2 fluxes measured with floating chambers (open circle) and from CH_4 fluxes measured with floating chambers (open triangle). (B) All data were considered and k_{600} were averaged over wind speed bins of 1 m s^{-1}. The solid line corresponds to this study relationship, and the long-dashed line corresponds to the Thames estuary relationship (T), the short-dashed line corresponds to the Scheldt Estuary relationship (S), and the dashed-dotted line to the Randers Fjord relationship (RF) from Borges et al. (2004a) and the fine solid line and dotted-dashed line correspond to Sage Pond River (SPR) and Childs River (CR) relationship, respectively, from Kremer et al. (2003b).

highest values of k_{600} when water was warmer than air or during periods following strong winds and rapidly falling temperature. During our measurements the average ΔT between water and air was 2.1 °C ranging from −2.2 °C to 6.7 °C, generating a cooling of the surface water by evaporation. Like Cole and Caraco (1998), we could however not find any significant correlation between the thermal gradient and the difference between the individual k_{600} and the "mean" k_{600} derived from our k_{600}–U relationship ($p=0.6085$). The large range of ΔT during our measurements can also explain the scatter of our low wind speed data.

In the tidal river downstream of the dam, the k_{600} values were 3 to 4 times higher than at the lake surface at the same wind speed (Table 2) due to the turbulence induced by water currents (Zappa et al., 2003; Borges et al., 2004a). In addition, the relationship with wind speed was steeper than in the lake. The whole dataset (Fig. 2A) presents a large scatter probably due to rapid changes in water current, water depth and bed roughness between individual measurements. The mean k_{600} in the Sinnamary Estuary was high (10.8 ± 6.4 cm h^{-1} $n=84$) which is consistent with previous studies in rivers and estuaries (Devol et al., 1987; Marino and Howarth, 1993; Clark et al., 1994; Frankignoulle et al., 1996a; Zappa et al., 2003; Borges et al., 2004a,b). On Fig. 2B, the whole dataset was averaged over wind speed bins of 1 m s^{-1}. The relation obtained is considered to be linear (Table 4) as shown in some other estuaries (Kremer et al., 2003b; Borges et al., 2004a). The difference of the formulation of the k_{600}-wind relationship from one site to another is still under debate. The most common hypothesis to explain these differences is that the slope of the linear regression could be due to the fetch limitation and the intercept to the contribution of water currents (Hartman and Hammond, 1984; Wanninkhof, 1992; Kremer et al., 2003b; Borges et al., 2004a). The fetch effect was shown in wind tunnel (Wanninkhof and Bliven, 1991) and in estuaries (Borges et al., 2004a). As shown in Fig. 3, the slope of the Sinnamary River k_{600}–U_{10} relationship (2.7 cm h^{-1}/m s^{-1}) fitted well with the formulation as a function of surface area proposed by Borges et al. (2004a).

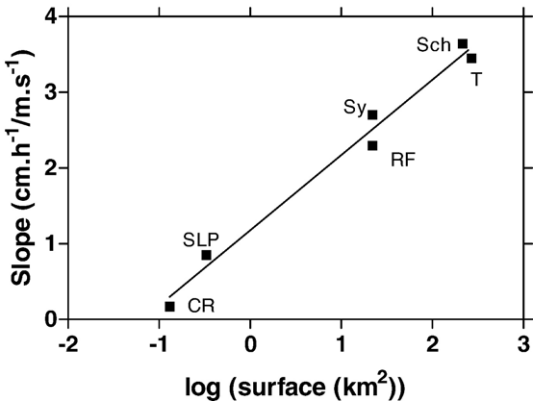

Fig. 3. Relationship between the slope of the linear regression functions of k_{600} versus wind speed and the Log of surface area in several estuaries, including the Sinnamary Estuary and tidal river (Sy, slope 2.7 cm h^{-1}/m s^{-1} and surface area 21 km^2), the Thames (T), Scheldt (Sch), Randers Fjord (RF), Childs River (CR), and Sage Lot Pond (SLP). Data for the Thames (T), Scheldt (Sch), and Randers Fjord (RF) Estuaries are from Borges et al. (2004a). Data for Childs River and Sage Lot Pond are from Kremer et al. (2003a), after the normalization to a Schmidt number of 600 made by Borges et al. (2004a), Solid line corresponds to model 1 regression function (slope=0.99 (±0.06 SE)+ 1.2 (±0.1 SE) log (surface area), $r^2=0.98$, $p<0.0001$, $n=6$).

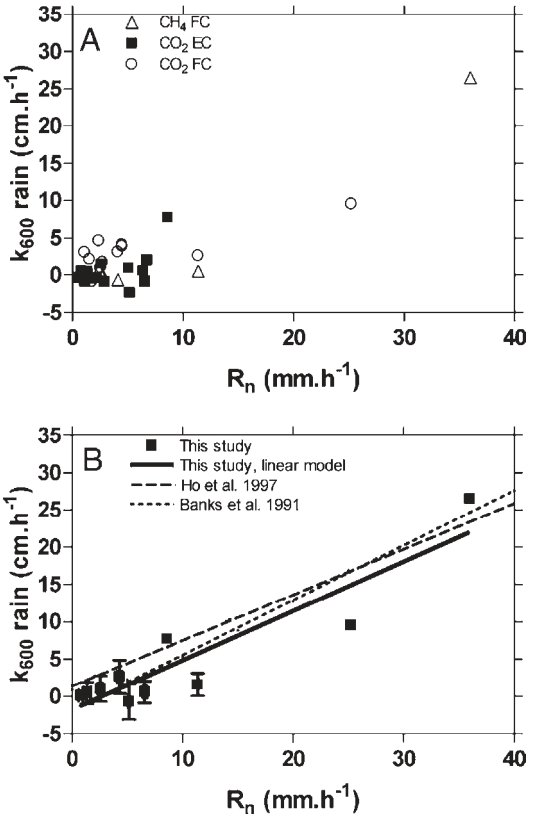

Fig. 4. (A) Residual normalized gas transfer velocities, k_{600}, plotted against mean rain rate R_n at the lake surface computed from CO_2 fluxes measured with floating chambers (open circle) and eddy covariance (solid square) and from CH_4 fluxes measured with floating chambers (open triangle). (B) All data were considered and k_{600} were averaged over wind speed bins of 1 mm h^{-1} (Solid Square). The solid line corresponds to this study relationship, and the long-dashed line corresponds to the Ho et al. (1997) relationship (H97), the short-dashed line corresponds to the Banks et al. (1984) relationship (B84).

3.4. Rainfall effect

Rain falling on a water body is another mechanism creating turbulence at the water surface and leading to an enhancement of the k_{600} (Banks et al., 1984; Ho et al., 1997). Quantification of this effect requires the wind influence to be removed from the data using our relationship between k_{600} and wind speed (Table 4). Therefore we calculated the difference between our k_{600} value during rainy events and our k_{600} without rainy events at the same wind speed (Cole and Caraco, 1998; Frost and Upstill-Goddard, 2002) (Table 4). The k_{600} dataset included rainfall rates from 0.6 to 36 mm h^{-1} with wind speeds from 0.1 to 3.3 m s^{-1}. The residual k_{600} was positively related to rainfall rates ($k_{600\ \mathrm{Rain}}=0.66\ (\pm0.10)\ R-1.81\ (\pm1.52)$, $r^2=0.84$, $p<0.0001$, $n=10$ for data averaged over rain rates bins of 1 mm h^{-1}) reaching 29 cm h^{-1} for a rainfall rate of 36 mm h^{-1} (Fig. 4). The fact that the effect of rainfall on k_{600} is measurable by the FC confirms that this method adequately picks up the effect of turbulence in the aquatic boundary layer on the gas transfer velocity. Our relationship is not statistically different from those obtained in laboratory experiments (Banks et al., 1984; Ho et al., 1997). The relationship of Ho et al. (1997) was obtained using a raindrop size distribution for a temperate rainfall (Marshall and Palmer, 1948). For rain rates lower than 10 mm h^{-1}, tropical rain have less raindrops with higher diameters (Sauvageot and Lacaux, 1995). Using their raindrop size distribution, we have calculated that tropical rain generates 20% more kinetics energy than temperate rain, for rainfall rates lower than 10 mm s^{-1}. For higher rainfall, tropical rain generates less turbulence than temperate rain. However, high temperature gradients between rain and lake waters probably generates a greater turbulence in tropical environments than in temperate environments. It is thus possible that the FCs slightly underestimates the k_{600} at very low rainfall rates at Petit Saut.

From the data in Figs. 1 and 4, the k_{600} of the Petit-Saut Lake can be written as:

$$k_{600} = 1.66(\pm0.34)\cdot e^{0.26(\pm0.04).U10} + 0.66(\pm0.10)R \quad (7)$$

The effect of precipitation is rarely taken into account in the gas emission estimations. Based on the annual mean precipitation at the Petit-Saut Reservoir (0.3 mm h^{-1}) and the Eq. (7), the impact of rainfall on the k_{600} of the Petit-Saut Lake is about 10% at the annual mean wind speed (1 m s^{-1}). During our 24-hour cycle in December 2003 (mean $U_{10}=1.7$ m s^{-1} and mean $R=1.3$ mm h^{-1}), rainfall accounted for about 25% of the k_{600}. Rainfall is therefore an important factor influencing the k_{600}, particularly in tropical environments where rainfall can reach 150 mm h^{-1}, that is, an instantaneous $k_{600\ \mathrm{Rain}}$ of about 100 cm h^{-1}.

4. Conclusions

The k_{600}-wind speed and k_{600}-rain rates relationships were obtained by comparing the k_{600} values obtained by the floating chambers and the eddy covariance techniques while measuring CO_2 and CH_4 fluxes at a tropical reservoir and its river downstream. At a given wind speed, both methods gave similar k_{600}. Thus, the FC appears to be a reliable and inexpensive technique to determine the gas transfer velocity in various environments (lakes, estuaries, rivers). To avoid the creation of artificial turbulence, chambers must however have walls extending into the water and measurements must be performed while drifting. In the Petit Saut Lake, the k_{600} dependence to wind speed followed an exponential model, with a significant intercept probably due to thermal effects. In addition, rainfall significantly contributes to the gas transfer velocity in such tropical environment. Finally, k_{600} was significantly higher in the river downstream of the dam than in the lake, due to a contribution of water current to the turbulence in the aquatic boundary layer.

Acknowledgments

The authors thank R. Aboïkoni and L. Guillemet for their assistance on the field, B. Burban and C. Reynouard for the laboratory and field assistance, J.-L. Fréchette for flux measurements and H. Sauvageot for rainfall kinetic energy flux calculation. This study was funded by the Electricité De France and the CNRS National Programs (PNCA and ECCO). We thank Alain Grégoire (EDF) for his continuous confidence. F.G. benefited from a PhD grant by EDF.

References

Abril, G., Guérin, F., Richard, S., Delmas, R., Galy-Lacaux, C., Tremblay, A., Varfalvy, L., Gosse, P., dos Santos, M.A., Matvienko, B., 2005. CH_4 and CO_2 emissions and carbon imbalance in a 10 years old tropical reservoir (Petit-Saut, French Guiana). Glob. Biogeochem. Cycles 19, doi:10.1029/2005GB002457.

Abril, G., Richard, S., Guérin, F., 2006. In-situ measurements of dissolved gases (CH_4 and CO_2) in a wide range of concentrations in a tropical reservoir using an equilibrator. Sci. Total Environ. 354, 246–251.

Affre, C., Lopez, A., Carrara, A., Druilhet, A., Fontan, J., 2000. The analysis of energy and ozone flux data from the LANDES 94 experiment. Atmos. Environ. 34, 803–821.

Amorocho, J., DeVries, J.J., 1980. A new evaluation of the wind stress coefficient over water surfaces. J. Geophys. Res. 85, 433–442.

Anderson, D.E., Striegl, R.G., Stannard, D.I., Michmerhuizen, C.M., 1999. Estimating lake-atmosphere CO_2 exchange. Limnol. Oceanogr. 44, 988–1001.

Banks, R.B., Wickramanayake, G.B., Lohani, B.N., 1984. Effect of rain on surface reaeration. J. Environ. Eng. 110, 1–14.

Beverland, I.J., Moncrieff, J.B., Ónéill, C., Hargreaves, K.J., Milne, R., 1996. Measurement of methane and carbon dioxide fluxes from peatland ecosystems by the conditional-sampling technique. Q. J. R. Meteorol. Soc. 122, 819–838.

Borges, A.V., Delille, B., Schiettecatte, L.-S., Gazeau, F., Abril, G., Frankignoulle, M., 2004a. Gas transfer velocities of CO_2 in three European estuaries (Randers Fjord, Scheldt and Thames). Limnol. Oceanogr. 49, 1630–1641.

Borges, A.V., Vanderborght, J.P., Schiettecatte, L.-S., Gazeau, F., Ferron-Smith, S., Delille, B., Frankignoulle, M., 2004b. Variability of the Gas Transfer Velocity of CO_2 in a Macrotidal Estuary (the Scheldt). Estuaries 27, 593–603.

Businger, J.A., 1986. Evaluation of the accuracy with which dry deposition can be measured with current micrometeorological techniques. J. Clim. Appl. Meteorol. 25, 1100–1124.

Clark, J.F., Wanninkhof, R., Schlosser, P., Simpson, H.J., 1994. Gas exchange in the tidal Hudson River using a dual tracer technique. Tellus 46B, 274–285.

Cole, J.J., Caraco, N.F., 1998. Atmospheric exchange of carbon dioxide in a low-wind oligotrophic lake measured by the addition of SF_6. Limnol. Oceanogr. 43, 647–656.

Crill, P.M., Bartlett, K.B., Wilson, J.O., Sebacher, D.I., Harriss, R.C., 1988. Tropospheric methane from an Amazonian floodplain lake. J. Geophys. Res. 93, 1564–1570.

Crucius, J., Wanninkhof, R., 2003. Gas transfer velocities measured at low wind speed over a lake. Limnol. Oceanogr. 48, 1010–1017.

Devol, A.H., Quay, P.D., Richey, J.E., Martinelli, L.A., 1987. The role of gas exchange in the inorganic carbon, oxygen, and ^{222}Rn budgets of the Amazon River. Limnol. Oceanogr. 32, 235–248.

Eugster, W., Kling, G., Jonas, T., McPhaden, J.P., Wüest, A., McIntyre, S., Chapin III, F.S., 2003. CO_2 exchange between air and water in an Arctic Alaskan and a midlatitude Swiss lake: importance of convective mixing. J. Geophys. Res. 108, doi:10.1029/2002JD002653.

Foken, T., Wichura, B., 1996. Tools for quality assessment of surface-based flux measurements. Agric. For. Meteorol. 78, 83–105.

Frankignoulle, M., Bourge, I., Wollast, R., 1996a. Atmospheric CO_2 fluxes in a highly polluted estuary (The Scheldt). Limnol. Oceanogr. 41, 365–369.

Frankignoulle, M., Gattuso, J.P., Biondo, R., Bourge, I., Copin-Montégut, G., Pichon, M., 1996b. Carbon fluxes in coral reefs. II. Eulerian study of inorganic carbon dynamics and measurement of air–sea CO_2 exchanges. Mar. Ecol., Prog. Ser. 145, 123–132.

Frankignoulle, M., Borges, A., Biondo, R., 2001. A new design of equilibrator to monitor carbon dioxide in highly dynamic and turbid environments. Water Res. 35, 1344–1347.

Frost, T., Upstill-Goddard, R.C., 2002. Meteorological controls of gas exchange at a small English lake. Limnol. Oceanogr. 47, 1165–1174.

Galy-Lacaux, C., Delmas, R., Kouadio, G., Richard, S., Gosse, P., 1999. Long-term greenhouse emissions from hydroelectric reservoirs in tropical forest regions. Glob. Biogeochem. Cycles 13, 503–517.

Hartman, B., Hammond, D.E., 1984. Gas exchange rates across the sediment–water and air–water interfaces in south San Francisco Bay. J. Geophys. Res. 89, 3593–3603.

Ho, D.T., Bliven, L.F., Wanninkhof, R., Schlosser, P., 1997. The effect of rain on air–water gas exchange. Tellus 49B, 149–158.

Hope, D., Dawson, J.J.C., Cresser, M.S., Billet, M.F., 1995. A method for measuring free CO_2 in upland streamwater using headspace analysis. J. Hydrol. 1666, 1–14.

Jähne, B., Munnich, K.O., Bosinger, R., Dutzi, A., Huber, W., Libner, P., 1987. On parameters influencing air–water exchange. J. Geophys. Res. 92, 1937–1949.

Kremer, J.N., Nixon, S.W., Buckley, B., Roques, P., 2003a. Technical note: conditions for using the floating chamber method to estimate air–water gas exchange. Estuaries 26, 985–990.

Kremer, J.N., Reischauer, A., D'Avanzo, C., 2003b. Estuary-specific variation in the air–water gas exchange coefficient for oxygen. Estuaries 26, 829–836.

Leuning, R., Judd, M.J., 1996. The relative merits of open-and closed-path analysers for measurement of eddy fluxes. Glob. Chang. Biol. 2, 241–253.

Liss, P.S., Slater, P.G., 1974. Flux of gases across the air–sea interface. Nature 233, 327–329.

Liss, P., Merlivat, L., 1986. Air–sea exchange rates: introduction and synthesis. In: Buat-Ménard, P. (Ed.), The Role of Air–Sea Exchanges in Geochemical Cycling. Reidel, Dordrecht, pp. 113–127.

Liss, P.S., Balls, P.W., Martinelli, F.N., Coantic, M., 1981. The effect of evaporation and condensation on gas transfer across an air–water interface. Oceanol. Acta 4, 129–138.

MacIntyre, S., Wanninkhof, R., Chanton, J.P., 1995. Trace gas exchange across the air–water interface in freshwaters and coastal marine environments. In: Matson, P.A., Harriss, R.C. (Eds.), Biogenic Trace Gases: Measuring Emissions from Soil and Water. Blackwell, pp. 52–97.

Mann, J., Lenschow, D.H., 1994. Errors in airborne flux measurements. J. Geophys. Res. 99, 519–526.

Marino, R., Howarth, R.W., 1993. Atmospheric oxygen-exchange in the Hudson River— dome measurements and comparison with other natural waters. Estuaries 16, 433–445.

Marshall, J.S., Palmer, W.M., 1948. The distribution of raindrops size. J. Meteorol. 5, 165–166.

Matthews, C.J.D., Saint-Louis, V.L., Hesslein, R.H., 2003. Comparison of three techniques used to measure diffusive gas exchange from sheltered aquatic surfaces. Environ. Sci. Technol. 37, 772–780.

McGillis, W.R., Edson, J.B., Ware, J.D., Dacey, J.W.H., Hare, J.H., Fairall, C.W., Wanninkhof, R., 2001. Carbon dioxide flux techniques performed during GasEx-98. Mar. Chem. 75, 267–280.

Raymond, P.A., Cole, J.J., 2001. Gas exchange in rivers and estuaries: choosing a gas transfer velocity. Estuaries 24, 312–317.

Saint Louis, V., Kelly, C., Duchemin, E., Rudd, J.W.M., Rosenberg, D.M., 2000. Reservoir surface as sources of greenhouse gases to the atmosphere: a global estimate. BioScience 20, 766–775.

Sauvageot, H., Lacaux, J.P., 1995. The shape of averaged drop size distributions. J. Atmos. Sci. 52, 1070–1083.

Stauffer, R.E., 1980. Windpower time series above a temperate lake. Limnol. Oceanogr. 25, 513–528.

Wanninkhof, R., 1992. Relationship between gas exchange and wind speed over the ocean. J. Geophys. Res. 97, 7373–7382.

Wanninkhof, R., Bliven, L., 1991. Relation between gas exchange, wind speed and radar backscatter in large wind-wave tank. J. Geophys. Res. 96, 2785–2796.

Wanninkhof, R., Ledwell, J.R., Broecker, W.S., 1985. Gas exchange wind speed relationship measured with sulfur hexafluoride on a lake. Science 227, 1224–1226.

Ward, B., Wanninkhof, R., McGillis, W.R., Jessup, A.T., DeGrandpre, M.D., Hare, J.E., Edson, J.B., 2004. Biases in the air–sea flux of CO_2 resulting from ocean surface temperature gradient. J. Geophys. Res. 109. doi:10.1029/2003JC001800.

Weiss, R.F., 1974. Carbon dioxide in water and seawater: the solubility of a non-ideal gas. Mar. Chem. 2, 203–215.

Yamamoto, S., Alcauskas, J.B., Crozier, T.E., 1976. Solubility of methane in distilled water and seawater. J. Chem. Eng. Data 21, 78–80.

Zappa, C., Raymond, P.A., Terray, E.A., McGillis, W.R., 2003. Variation in surface turbulence and the gas transfer velocity over a tidal cycle in a macro-tidal estuary. Estuaries 26, 1401–1415.